Ultrasonic-assisted Method of Graphite Preparation from Wheat Straw

Ming Xu, Liyan Xing, Qinqin Zhang, and Junwen Pu *

Graphite production was achieved unexpectedly in the course of demonstrating a new ultrasonic-assisted wheat straw pulping method at room temperature and at atmospheric pressure. The graphite material was found in the ultrasonic-assisted pulp (UP) ash, as shown by X-ray diffraction, Raman spectroscopy, X-ray photoelectron spectroscopy, and TEM analysis. UP ash contained both inorganic and organic components. The total content of inorganic components in the ash was 81.9%, while the content of organic component (graphite material) was 18.1%. The graphite content in the pulp was calculated to be approximately 4.5%. This work describes a new meaningful approach for the facile preparation of graphite materials. The graphitization was based on the ultrasonic cavitation mechanism of extreme condition, while the process would be divided into three steps, degradation of lignin, graphene formation, and graphitization process.

Keywords: Graphitization; Lignin; Ultrasonic-assisted pulp; Cavitation

Contact information: Ministry of Education (MOE) Engineering Research Center of Forestry Biomass Materials and Bioenergy, Beijing Forestry University, Beijing, 100083, China;
** Corresponding author: 13681243864@126.com*

INTRODUCTION

Graphite is an allotrope of carbon. As a natural inorganic non-metallic material, graphite is generally formed in high temperature geological conditions. It is widely distributed in the metamorphic deposit of sedimentary rocks rich in organic matter. The physical and chemical properties of graphite are reflective of two kinds of chemical bonds. The heat resistance and chemical stability are mainly derived from the σ bond, while the excellent electrical conductivity and lubricity property are coming from the π bond.

Conductive carbons, based on achieving a higher degree of graphite material, to prepare graphene or sensor materials, could be obtained from wood or crop straw *via* a thermo method, and has been attracting a great deal of attention due to their environmentally friendly properties (Pandolfo and Hollenkamp 2006; Wilson *et al.* 2007; Liang *et al.* 2015; Ni *et al.* 2015; Naseem *et al.* 2016; Ramesh 2016). The graphitizing process is the transformation from an amorphous and disordered layer structure of carbon materials into three-dimensional ordered graphite crystals. During this transition, the cross bond between the carbon atoms is disconnected, the apparent crystallite size of the six corner-net-plan is increased, and the interval D002 between the six corner-networks is reduced (Ma *et al.* 2012; Focke *et al.* 2014; Inagaki *et al.* 2014; Li *et al.* 2016).

The phase transition process requires high energy so that the graphite carbon can be deposited. Yoon *et al.* (2005) synthesized ordered macroporous carbon with a graphite structure *via* pyrolysis of mesophase pitch, with a pyrolysis temperature of 2500 °C. Hanzawa *et al.* (2002) obtained good graphite structure through pyrolysis of porous

carbon, with temperatures higher than 2000 °C. Catalytic graphitization by adding a transition metal, for example Fe-Si alloy, Ni-Cr alloy, or Fe_2O_3, Fe_3O_4, *etc.*, has become the most common method and can obtain higher degree graphitization carbon materials. But the temperature of catalytic graphitization is also very high and not well suited for industrial use (Endo *et al.* 2003; Lanticse-Diaz *et al.* 2009; Hawelek *et al.* 2016).

As mentioned, those methods with excessive energy consumption are challenging to implement on an industrial scale while maintaining good properties and avoiding high costs. Thus, ultrasonic technology has a bright prospect. The ultrasonic wave, a high-frequency mechanical wave, comes from a transducer that is usually made from piezoelectric crystal. The ultrasonic wave is also composed of a series of spaced longitudinal waves that spread through and interact with the liquid medium, leading to changes in the phase and amplitude, then impacting the medium state, composition, structure, and function, which are called ultrasonic effects (Yang and Wang 2008; Uchino 2012; Pardo 2015).

Mechanical, thermal, and cavitation mechanisms are the three important ultrasonic effects. The mechanical energy can cause alternating compression and extension of the medium; meanwhile a thermal effect is produced throughout the material (Watson *et al.* 2009; Chen *et al.* 2010). Acoustic cavitation is the main mechanism of the ultrasonic effect, including generation and movement of cavitation bubbles, which experience repetitive cycles of growing up, breaking, and growing up again. When the bubbles finally crack, at approximately 4000 K, 100 MPa pressure, and 110 m/s, a strong micro jet can be generated, which leads to the dissociation of water into hydroxyl free radicals (HO·) and hydrogen atoms. Furthermore, the resultant free radicals (HO·) can be transformed into H_2O_2 or HO_2·, which also have important oxidation capabilities (Makino *et al.* 1982; Christman *et al.* 1987).

Some researchers have realized that an ultrasonic technique could be a sufficient or supplementary method of the stalk materials treatment instead of chemical reaction, mechanical grinding, or pyrolysis. The considerable huge energy coming from an ultrasonic cavitation effect could contribute to the separation of the fibers and the degradation, or changing the crystalline degree of the material (Sheshin 2003; Koutsianitis *et al.* 2015; Villa-Vélez *et al.* 2015; He *et al.* 2017).

This study investigated an ultrasonic-assisted pulping method from wheat straw in a liquid media. Furthermore, the ultrasonic wave as a main energy endows an innovative graphitization process with a mild condition at normal temperature and atmospheric pressure.

EXPERIMENTAL

Materials

Wheat straw was obtained from the Shandong province of China and cut into small pieces (2 cm to 3 cm). Then the straw was processed with an ultrasonic reaction in an ultrasonic reactor (self-made, 5-L volume, Fig. 1), at the mass concentration of 10% to 15%, with a frequency of 16 kHz to 20 kHz at atmospheric pressure. Then the material was ultrasonically reacted for 30 min, followed by resting for 15 min. This was repeated for a total of three times, while the constant stirring speed was 500 rpm. Meanwhile, the chemical additives used in the reaction consisted of 5% ammonia, 0.5% sodium

dodecylsulphate, 3.5% silicate, 1.5% magnesium sulfate, in which the dosage was relative to dry raw materials.

As the control sample, the wheat straw was pulped in a lab digester reactor (Sinopaper Research Institute, Beijng, China) at a mass concentration of 20%, a peak temperature of 150 °C, heated for 60 min, with a holding time of 30 min, and the speed of autorotation was 10 rpm. The chemicals were NaOH 15%, anthraquinone 0.5%, in which the dosage was relative to the dry raw materials. All chemicals (Sinopharm Chemical Reagent Co., Ltd., Shanghai, China) were commercial products and used as received.

The ultrasonic assisted pulp (UP) and alkali pulp (AP) were washed and screened with a 0.15-mm slot screen.

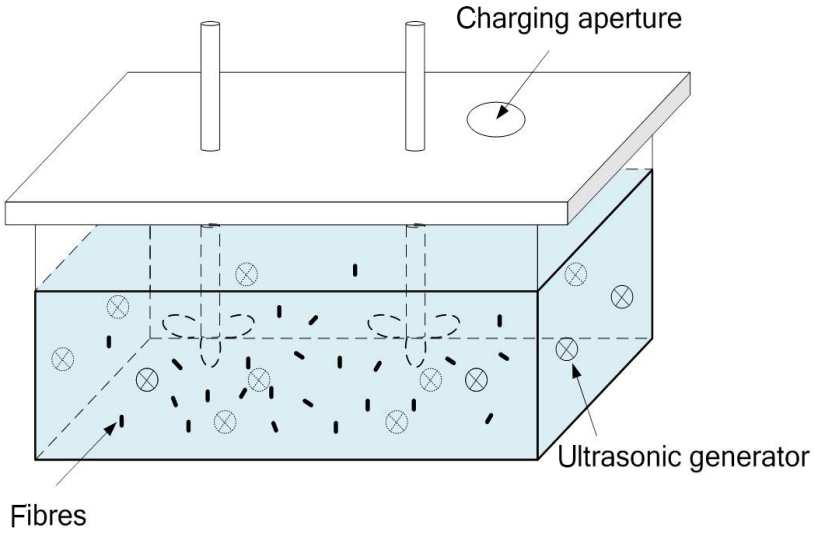

Fig. 1. Ultrasonic reaction device

The method for the preparation of residual lignin was outlined in the previous literature (Pew 1957). The UP and AP were milled (Taisite Instrument Co., Ltd., Tianjin, China) and ground for 10 h in a porcelain ball grinder (Changsha MITR Instrument Equipment Co., Ltd., Changsha, China). Then, 100 g of the ground pulp meal was conducted to an enzyme treatment for 72 h with cellulase, which contained a small amount of hemicellulase. The enzymatic hydrolysis was performed at a consistency of 300 units/g oven-dried pulp in a water bath shaker (Taicang Hualida Experiment Equipment Co., Ltd., Shanghai, China), which was set at 40 °C and 240 rpm. The resulting crude residual lignin was freeze-dried after being washed twice with acidic deionized water (pH = 2.0).

Next, the crude lignin was suspended in 100 mL of acidic dioxane-water (85:15 v/v) and was refluxed (boiling point of 86 °C) under nitrogen protection for 2 h and then filtered. The resulting solid was washed with fresh dioxane-water (85:15 v/v) until the filtrate was clear. All of the filtrated lignin solutions were combined and neutralized with sodium bicarbonate, and then the mixture was rotary evaporated at 30 °C. The concentrated syrup-like solution was added drop by drop to a large quantity of acidified deionized water and placed overnight. The precipitated lignin was isolated by centrifugation, washed with deionized water, and then freeze-dried. The lignin was lastly washed with high-pressure liquid chromatography (HPLC) grade hexane and dried in a vacuum oven at room temperature.

Methods

The thermal behavior of pulp was explored using a thermal analyzer (STA449, Netzsch, Selb, Germany). The thermogravimetric curves were obtained at 50 °C to 500 °C in air atmosphere with a heating rate of 10 °C/min.

The X-ray diffraction (Shimadzu model XRD 6000, Kyoto, Japan) analysis was performed, while the scanning speed, step size, and scanning ranges were 0.5 s/step, 0.04°, and 5° to 60°, respectively.

Raman spectra were collected from $500 \sim 2000 cm^{-1}$ using a micro-Raman spectrometer (LabRam 300, HORIBA Jobin Yvon, Paris, France) with an excitation wavelength of 633 nm.

TEM images were analyzed from the transmission electron microscope (JEM-1010, JEOL, Tokyo, Japan) after the pretreatment of dispersion in the alcohol and drying.

The inorganic elements were measured by a plasma emission spectrometer (ICP-OES icap6300, Thermofisher, Waltham, USA). The main working parameters were: plasma power, 1150 W; gas flow rate, 0.6 L/min; auxiliary gas flow, 0.5 L/min; and peristaltic pump speed, 50 rpm.

The elements species were determined by an electron spectrometer (Escalab Mk II, VG Instruments Inc., London, UK); the chamber vacuum maintenance was more than 5×10^{-10} mbar, with the accelerating voltage of 12 kV, and an operating current of 14 mA.

The content analysis of H was performed by an elemental analyzer (Vario macro, Elementar Instruments Inc., Hanau, Germany), with an auxiliary gas of high purity oxygen and a carrier gas of high purity helium.

RESULTS AND DISCUSSION

From the results of the author's previous research (Xing *et al.* 2017), it was demonstrated that many protrusion spherical granular materials were present on the fiber surface of UP, and the pulp had commendable strength performances. Meanwhile, the ash content of UP reached 27.8%, which was far higher than that of the traditional wheat straw pulp. Especially from the XRD analysis, there was a clear peak at $2\theta = 26.5°$ on the curve of UP that was not present for traditional wheat straw pulp. This provoked a desire to explore further.

Thermogravimetric Analysis

The components of the pulp can be studied further by thermal degradation properties. The thermogravimetric analysis of UP and AP lignin was conducted, the curves are shown in Fig. 2. The figure shows that a small amount of mass loss of both samples occurred before 100 °C and was due to the evaporation of water. Rapid decomposition of both samples happened from 240 °C to 480 °C, which was mainly from the thermal degradation of organic molecules that contained H and C. The maximum loss of quantity corresponded to 310 °C. The range of the mass loss of UP lignin was much smaller than the AP lignin. In AP lignin curve (b), the weight loss trend became almost stable after 480 °C, and the residue was only approximately 3%. However, the trend was different from the curve of UP lignin (a), in which the weight loss looks like it decreased continuously. At 800 °C, the residue weight also remained approximately 24%. This further offered a valuable ratiocination that the high temperature resistant material would

be contained in or come from the lignin of ultrasonic pulp, and seems related to the structural unit of benzene propane.

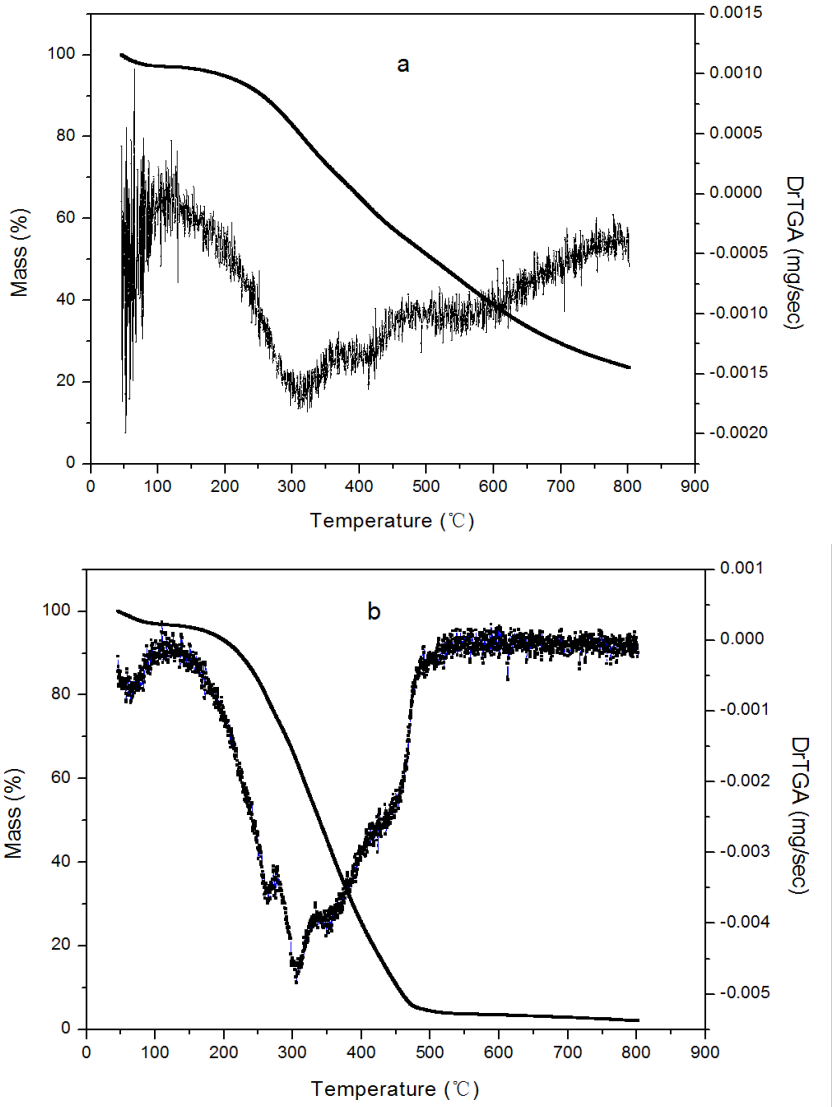

Fig. 2. Thermal analysis curves of UP (a) and AP (b) lignin

XRD

To clarify the above problems, another X-ray diffraction analysis of UP ash sample after 575 °C combustion was performed. The X-ray diagram is shown in Fig. 3.

The only large and clear diffraction peak without interference appeared at 2θ = 26.6807°. While taking into account that there were critical partial conditions in the ultrasonic reaction (4000 K temperature, 100 MPa pressure), the authors concluded that the crystal composition was graphite crystal. The interlayer distance was calculated according to Eq. 1,

$$d_{002}=\lambda/(2sin\theta) \quad (1)$$

where λ is the X-ray wavelength and θ is the 002 surface diffraction angle. When λ = 1.54056×10^{-10}m and 2θ = 26.6807°, the d_{002} = 0.3339 nm.

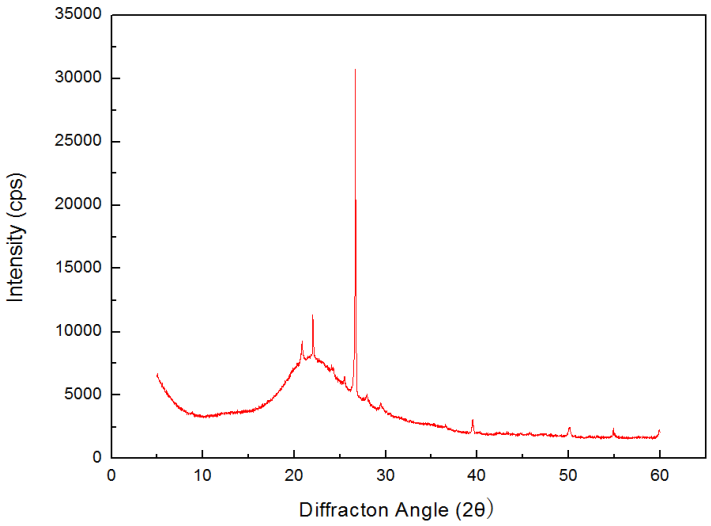

Fig. 3. XRD of UP ash

The value of d_{002} (0.3339nm) was very close to that of graphite, which indicated the graphitizing level was relatively high. While the interlayer distance of the graphite crystal was much less than the sample obtained by high temperature and high pressure in many publications (Iwashita *et al.* 2004; Mirza-Aghayan *et al.* 2016). The result also corresponded to the fact that the degree of crystallization of UP was more than AP. In addition, the degree of crystallization of the UP ash was 25.3%, which could have also supported the above result.

Raman Analysis

Raman spectrum of UP ash is shown in Fig. 4. The components of the ash sample were complicated, although the fluorescence background signal was strong, two previously reported and prominent bands occurred; one is G band at 1573 cm^{-1}, attributed to polyaromatic structures of graphite C-C with crystal symmetry, another is D band at 1340 cm^{-1}, referred to as the defect band (Angoni 1993).

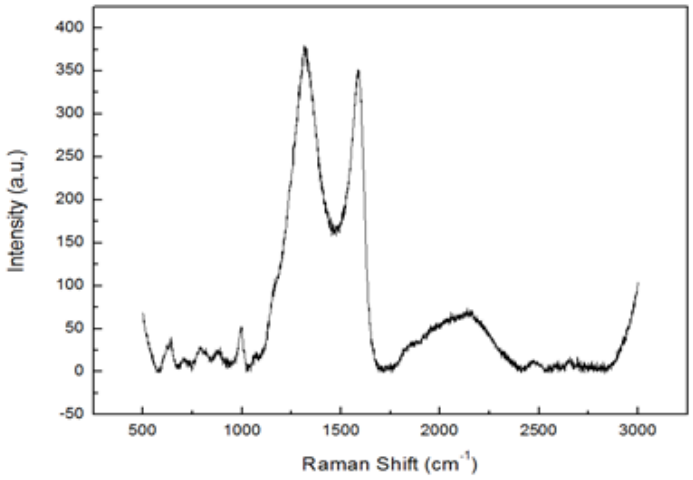

Fig. 4. Raman Spectrum of UP ash

The ratio of intensities of I_D/I_G was calculated to be 1.06, indicating the presence of graphite material in the ash sample, which means that more carbon with sp^2

hybridization occurred, and coincided with the XRD results. But the value of I_D/I_G is above 1, demonstrating the graphitization degree is not high enough. Further study needs to be conducted so as to achieve a high degree graphitization carbon from ultrasonic method.

TEM

In order to confirm the existence of the graphite material, a transmission electron microscopy (TEM) image (Fig. 5) was also obtained, and more details were demonstrated. Some thin layer materials were observed in the UP ash sample, which had regular shapes or folds. The side length of the rectangular thin layer was around 50 nm, illustrated that these images are rather probably representative of graphite like materials. Of course, the cross-section images of these materials should also be measured later.

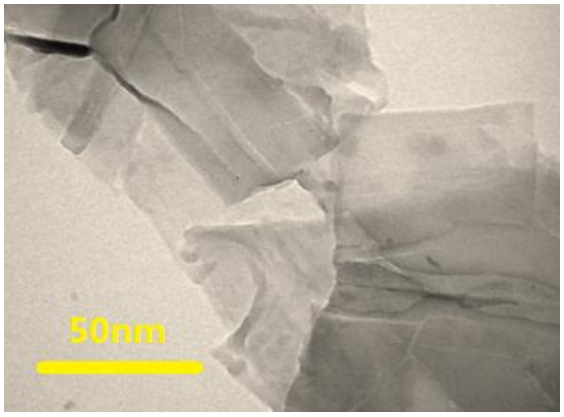

Fig. 5. TEM image of UP ash

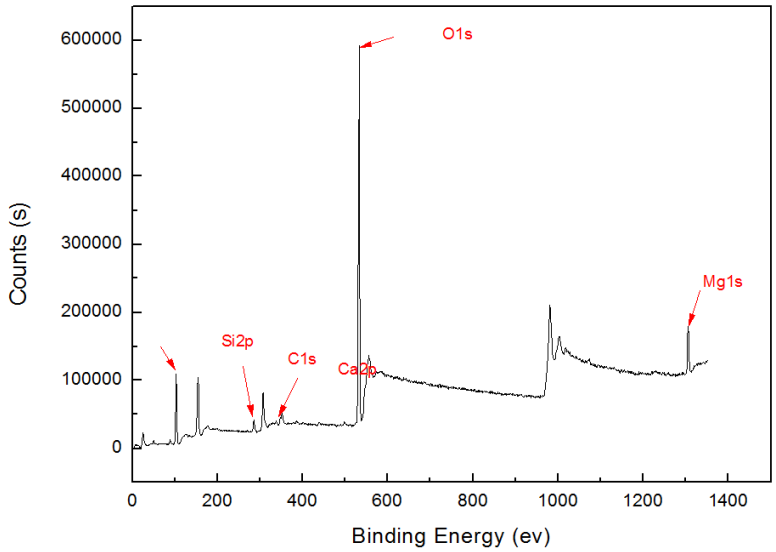

Fig. 6. XPS of UP ash

X-ray Photoelectron Spectroscopy

To measure the content of graphite material in the pulp, the ash sample was determined *via* X-ray photoelectron spectroscopy (XPS). The XPS spectrum is shown in Fig. 6. As can be seen, C, O, Si, Mg, and Ca were the main elements included in the ash,

with the highest content being O at 48.7%, followed by Si, 33.6%. Carbon was found in the ash, whose content was 12.0%, that is to say that some components that contained element C indeed were present in the pulp ash. The graphite or graphite similarly lamellar structure materials, which did not burn but was retained in the ash, were confirmed as being produced in the ultrasonic-assisted process.

Elemental Analysis

For further quantitative investigation, the inorganic ions content of UP ash were measured by ICP, the element content of H was obtained by the element analyzer, and the comprehensive results are reported in Table 1.

Table 1. Elements and Oxide Contents in UP Ash

Elements	Content (%)	Oxide	Content (%)
C	12.05	Graphite-Oxide	18.12
H	0.65		
Si	33.55	SiO_2	71.89
Mg	1.65	MgO	2.75
Ca	1.74	CaO	2.44
Al	0.52	Al_2O_3	1.96
Na	0.51	Na_2O	1.37
Fe	0.32	Fe_3O_4	1.00
K	0.19	K_2O	0.46
O	48.68	-	-
Total	99.86	-	100

Table 1 shows the element types and contents in the ash and their probability oxide contents. Different from traditional fiber samples, the ash (noncombustible components) of UP contained both inorganic and organic components. The total content of inorganic components was 81.9%, in which the content of SiO_2 was the highest, 71.9%, while the oxides in descending order were MgO (2.8%), CaO (2.4%), Al_2O_3 (1.96%), Na_2O (1.37%), Fe_3O_4 (1.00%), and K_2O (0.46%).

The organic component was graphite material, whose content was 18.12%, and the ratio of the C, H, and O elements mass contents was about 12.05:0.65:5.28, respectively. Considering the ash content was 24.9%, it could have been calculated that the graphite oxide content in the pulp fiber was approximately 4.5%, which indicated that there were certain amounts of lignin converted to graphite being on or in the fibers and increased the pulp yield.

Exploring the Mechanism of Graphitization

Although the graphitization degree seems not high, the generation of graphite and similarly structure materials was confirmed. It notable that phonochemistry accompanied by transient extreme temperature (4000 K), and pressure (100 MPa) played a great significant role in the pulping and graphitization process, which comes mainly from cavitation effect occurred in the gas-solid-liquid interface.

The graphitization process generally can be divided into three steps. Degradation of lignin is the first step, in which the β-O-4, α-O-4, and β-β chemical bonds were fractured, and the network structure of lignin in intercellular layer and corner layer were destroyed, making large molecular network structure gradually into small one; while the fibers were separated to form pulp (Fig. 7) (Hoflman *et al.*1996; Hamdaoui and Naffrechoux 2008). The degradation of chemical compounds by acoustic cavitation is shown to involve three distinct pathways: 1) oxidation by hydroxyl radicals (•OH or •OOH), 2) pyrolytic decomposition, and 3) supercritical water oxidation (Contamine *et al.*1994; Henglein 1995).

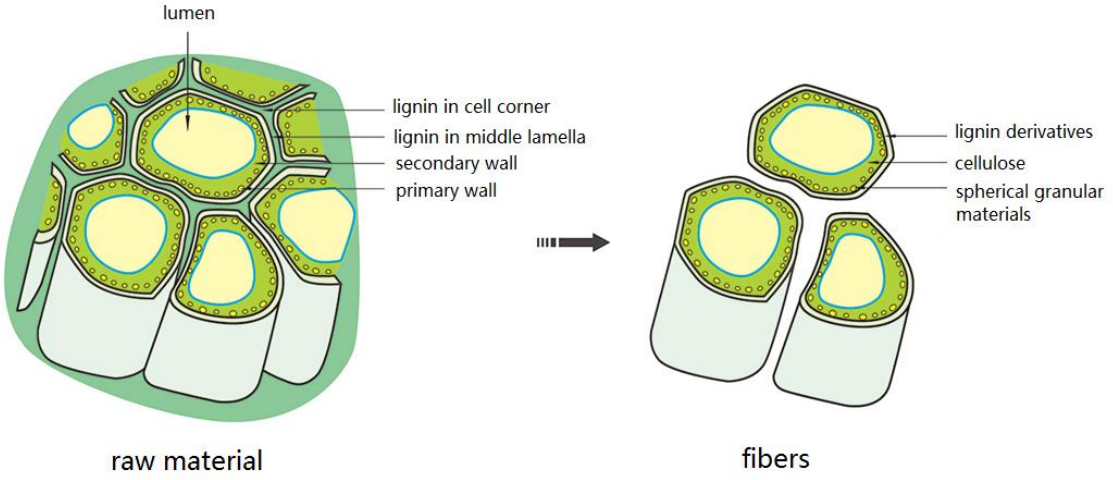

Fig. 7. Diagram of degradation of lignin and pulping

Next, low molecule acids, alcohol or ester materials are split off from the smaller lignin molecules, and some benzene hydrocarbons gradually accumulate, and they will be increasingly close to each other. Then in the boundary extreme conditions, condensation and dehydrogenation of the benzene hydrocarbon takes place and graphene layers form and grown (Hoflman *et al.*1996; Mirza-Aghayan *et al.* 2016).

The third step is a graphitization process, in which the disorganized graphene layers undergo self-assembly to overlap each other. In this manner, the graphitic carbon would precipitate on the fiber due to the driving force of a decreasing energy level. At last, a plurality of graphene layers is changed into crystalline graphite, at which point the graphitization process is basically complete, as shown in Fig. 8 (Laughrey*et al.* 2001; Simin *et al.* 2017).

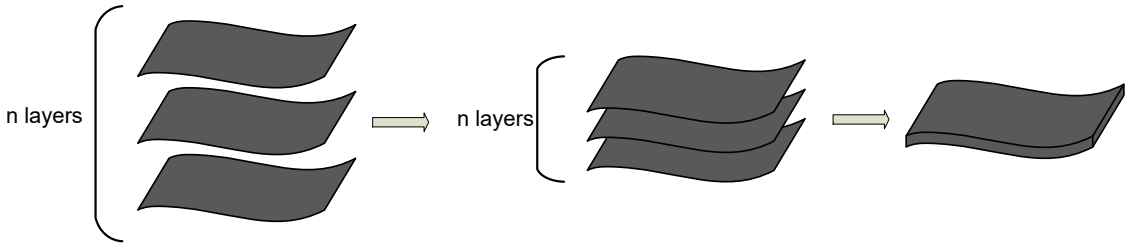

Fig. 8. Diagram of graphitization process

CONCLUSIONS

1. A novel ultrasonic-assisted wheat straw pulping method at room temperature and at atmospheric pressure was demonstrated. Graphite material was found unexpectedly in the ultrasonic-assisted pulp (UP), as shown by X-ray diffraction, Raman spectroscopy, X-ray photoelectron spectroscopy, and TEM analysis.
2. UP ash contained both inorganic and organic components. The total content of inorganic components was 81.9%, in which SiO_2 had the maximum content, 71.9%. The content of organic component (graphite material) was 18.1%, and the ratio of the C, H, and O elements mass contents was 12.0, 0.65, and 5.28 respectively, while the graphite content in the pulp was approximately 4.5%.
3. The graphitizing method was based on the ultrasonic cavitation effect with the cavitation bubbles cracking atmosphere approximately 4000 K temperature and 100 MPa pressure. The graphitization process would be mainly divided into three steps, degradation of lignin, graphene formation and graphitization process.

ACKNOWLEDGEMENTS

This work was sponsored by the Special Fund for the Beijing Common Construction Project and Beijing Forestry University, Grant No. 2016HXKFCLXY0016.

REFERENCES CITED

Angoni, K. (1993). "Remarks on the structure of carbon materials on the basis of Raman spectra," *Carbon* 31(4), 537-547. DOI: 10.1016/0008-6223(93)90106-K

Chen, J. Y., Chen, Y. Z., Li, H. L., Lai, S. Y., and Jow, J. (2010). "Physical and chemical effects of ultrasound vibration on polymer melt in extrusion," *Ultrasonics Sonochemistry* 17(1), 66-71. DOI: 10.1016/j.ultsonch.2009.05.005

Christman, C. L., Carmichael, A. J., Mossoba, M. M., and Riesz, P. (1987). "Evidence for free radical produced in aqueous solutions by diagnostic ultrasound," *Ultrasonics* 25(1), 31-34. DOI: 10.1016/0041-624X(87)90008-4

Contamine, F., Faid, F., Wilhelm, A. M., Berlan, J., and Delmas, H. (1994). "Chemical reactions under ultrasound: discrimination of chemical and physical effects," *Chemical Engineering Scienc*e 49(24), 5865-5873. DOI: 10.1016/0009-2509(94)00297-5

Endo, M., Kim, Y. A., Hayashi, T., Yanagisawa, T., Muramatsu, H., Ezaka, M., Terrones, H., Terrones, M., and Dresselhaus, M. S. (2003). "Microstructural changes induced in "stacked cup" carbon nanofibers by heat treatment," *Carbon* 41(10), 1941-1947. DOI: 10.1016/S0008-6223(03)00171-4

Focke, W. W., Badenhorst, H., Ramjee, S., Kruger, H. J., Schalkwyk, R. V., and Rand, B. (2014). "Graphite foam from pitch and expandable graphite," *Carbon* 73(14), 41-50. DOI: 10.1016/j.carbon.2014.02.035

Hamdaoui, O., and Naffrechoux, E. (2008). "Sonochemical and photosonochemical degradation of 4-chlorophenol in aqueous media," *Ultrasonics Sonochemistry* 15(6), 981-987. DOI: 10.1016/j.ultsonch.2008.03.011

Hanzawa, Y., Hatori, H., and Yoshizawa, N., and Yamada, Y. (2002). "Structural changes in carbon aerogels with high temperature treatment," *Carbon* 40(4), 575-581. DOI: 10.1016/S0008-6223(01)00150-6

Hawelek, L., Wlodarczyk, P., Hudecki, A., Lis, M., Zackiewicz, P., Jurkiewicz, K., Szade, J., Kubacki, J., Balin, K., Fischer, H. E., Kolano-Burian, A., and Burian, A. (2016). "The atomic scale structure of glass-like carbon obtained from fullerene extract *via* spark plasma sintering," *Carbon* 110(9), 172-179. DOI: 10.1016/j.carbon.2016.09.017

He, Z., Wang, Z., Zhao, Z., Yi, S., Mu, J., and Wang, X. (2017). "Influence of ultrasound pretreatment on wood physiochemical structure," *Ultrasonics Sonochemistry* 34(1), 136-141. DOI: 10.1016/j.ultsonch.2016.05.035

Henglein, A. (1995). "Chemical effects of continuous and pulsed ultrasound in aqueous solutions," *Ultrasonics Sonochemistr*y 2(2), 115-121. DOI: 10.1016/1350-4177(95)00022-X

Hoflman, M. R., Hua, I., and Höchemerm R. (1996). "Application of ultrasonic irradiation on for the degradation of chemical contaminants in water," *Ultrasonics Sonichemistr*y 3(3), 163-172. DOI: 10.1016/S1350-4177(96)00022-3

Inagaki, M., and Kang, F. (2014). "Engineering and applications of carbon materials," in: *Materials Science and Engineering of Carbon: Fundamentals (Second Edition)*, M. Inagaki, and F. Kang (eds.), Butterworth-Heinemann, Waltham, MA, pp. 219-525. DOI: 10.1016/B978-0-12-800858-4.00003-6

Iwashita, N., Park, C. R., Fujimoto, H., Shiraishi, M., and Inagaki, M. (2004). "Specification for a standard procedure of X-ray diffraction measurements on carbon materials," *Carbon* 42(10), 701-704. DOI: 10.1016/j.carbon.2004.02.008

Koutsianitis, D., Mitani, C., Giagli, K., Tsalagkas, D., Halász, K., Kolonics, O., Gallis, C., and Csóka, L. (2015). "Properties of ultrasound extracted bicomponent lignocellulose thin films," *Ultrasonics Sonochemistry* 23(3), 148-155. DOI: 10.1016/j.ultsonch.2014.10.014

Lanticse-Diaz, L. J., Tanabe, Y., Enami, T., Nakamura, K., Endo, M., and Yasuda, E. (2009). "The effect of nanotube alignment on stress graphitization of carbon/carbon nanotube composites," *Carbon* 47(4), 974-980. DOI: 10.1016/j.carbon.2008.11.046

Laughrey, Z., Bear, E., Jones, R., and Tarr, M. A. (2001). "Aqueous sonolytic decomposition of polycyclic aromatic hydrocarbons in the presence of additional dissolved species," *Ultrasonics Sonichemistry* 8(4), 353-357. DOI: 10.1016/S1350-4177(00)00080-8

Li, P. P., Zheng, Y. P., Li, M. Z., Shi, T., Li, D., and Zhang, A. B. (2016). "Enhanced toughness and glass transition temperature of epoxy nanocomposites filled with solvent-free liquid-like nanocrystal-functionalized graphene oxide," *Materials & Design* 89(1), 653-659. DOI: 10.1016/j.matdes.2015.09.155

Liang, X. T., Qu, B., Li, J. R., Xiao, H. N., He, B. H., and Qian, L.Y. (2015). "Preparation of cellulose-based conductive hydrogels with ionic liquid," *Reactive and Functional Polymers* 86(1), 1-6. DOI: 10.1016/j.reactfunctpolym.2014.11.002

Ma, Z. K., Liu, L., Lian, F., Song, H. H., and Liu, J. (2012). "Three-dimensional thermal conductive behavior of graphite materials sintered from ribbon mesophase pitch-based fibers," *Materials Letters* 66(1), 99-101. DOI: 10.1016/j.matlet.2011.08.024

Makino, K., Mossoba, M. M., and Riesz, P. (1982). "Chemical effects of ultrasound on aqueous solutions. Evidence for hydroxyl and hydrogen free radicals (·OH and ·H) by

spin trapping," *Journal of the American Chemical Society* 104(12), 3537-3539. DOI: 10.1021/ja00376a064

Mirza-Aghayan, M., Ganjbakhsh, N., Tavana, M. M., and Boukherroub, R. (2016). "Ultrasound-assisted direct oxidative amidation of benzyl alcohols catalyzed by graphite oxide," *Ultrasonics Sonochemistry* 32, 37-43. DOI: 10.1016/j.ultsonch.2016.02.017

Naseem, A., Tabasum, S., Zia, K. M., Zuber, M., Ali, M., and Noreen, A. (2016). "Lignin-derivatives based polymers, blends and composites: A review," *International Journal of Biological Macromolecules* 93(12), 296-313. DOI: 10.1016/j.ijbiomac.2016.08.030

Ni, J. F., Zhang, L., Fu, S. D., Savilov, S. V., Aldoshin, S. M., and Lu, L. (2015). "A review on integrating nano-carbons into polyanion phosphates and silicates for rechargeable lithium batteries," *Carbon* 92(10), 15-25. DOI: 10.1016/j.carbon.2015.02.047

Pandolfo, A. G., and Hollenkamp, A. F. (2006). "Carbon properties and their role in supercapacitors," *Journal of Power Sources* 157(1), 11-27. DOI: 10.1016/j.jpowsour.2006.02.065

Pardo, L. (2015). "Piezoelectric ceramic materials for power ultrasonic transducers," in: *Power Ultrasonics*, J. A. Gellego-Juárez, K. F. Graff (eds.), Woodhead Publishing, Cambridge, UK, pp. 101-125. DOI: 10.1016/B978-1-78242-028-6.00005-3

Pew, J. C. (1957). "Properties of powdered wood and isolation of lignin by cellulytic enzymes," *TAPPI* 40(7), 553-558.

Ramesh, M. (2016). "Kenaf (*Hibiscus cannabinus* L.) fibre based bio-materials: A review on processing and properties," *Progress in Materials Science* 78(6), 1-92. DOI: 10.1016/j.pmatsci.2015.11.001

Sheshin, E. P. (2003). "Properties of carbon materials, especially fibers, for field emitter applications," *Applied Surface Science* 215(6), 191-200. DOI: 10.1016/S0169-4332(03)00275-7

Simin, N., Amir, H., M., Mahdi, S., Kamyar,Y., Ramin, N., Mahmood A., and Gholam H., S. (2017). "Degradation kinetics of tetracycline in aqueous solutions using peroxydisulfate activated by ultrasound irradiation: Effect of radical scavenger and water matrix," *Journal of Molecular Liquids* 241, 704-714. DOI: 10.1016/j.molliq.2017.05.137

Uchino, K. (2012). "Piezoelectric ceramics for transducers," in: *Ultrasonic Transducers*, K. Nakamura (ed.), Woodhead Publishing, Cambridge, UK, pp. 70-116. DOI: 10.1533/9780857096302.1.70

Villa-Vélez, H. A., Váquiro, H. A., and Telis-Romero, J. (2015). "The effect of power-ultrasound on the pretreatment of acidified aqueous solutions of banana flower-stalk: Structural, chemical, and statistical analysis," *Industrial Crops and Products* 66(4), 52-61. DOI: 10.1016/j.indcrop.2014.12.022

Watson, B., Friend, J., and Yeo. L. (2009). "Piezoelectric ultrasonic micro/milli-scale actuators," *Sensors and Actuators A: Physical* 152(2), 219-233. DOI: 10.1016/j.sna.2009.04.001

Wilson, S. A., Jourdain, R. P. J., Zhang, Q., Dorey, R. A., Bowen, C. R., Willander, M., Wahab, Q. U., Willander, M., Safaa, M. A., Nur, O. *et al.* (2007). "New materials for micro-scale sensors and actuators: An engineering review," *Materials Science and Engineering: R: Reports* 56(1-6), 1-129. DOI:10.1016/j.mser.2007.03.001

Xing, L. Y., Xu, M., and Pu, J. W. (2017). "The properties and application of an ultrasonic wheat straw pulp having enhanced tendency for ash formation," *BioResources* 12(1), 871-881. DOI: 10.15376/biores.12.1.871-881

Yang, J. S., and Wang, J. (2008). "Dynamic anti-plane problems of piezo ceramics and applications in ultrasonics – A review," *Acta Mechanica Solida Sinica* 21(3), 207-220. DOI: 10.1007/s10338-008-0824-3

Yoon, S. B., Chai, G. S., Kang, S. K., Yu, J. S., Gierszal, K. P., and Jaroniec, M. (2005). "Graphitized pitch-based carbons with ordered nanopores synthesized by using colloidal crystals as templates," *Journal of American Chemical Society* 127(12), 4188-4189. DOI: 10.1021/ja0423466

Article submitted: December 23, 2016; Peer review completed: March 18, 2017; Revised version received and accepted: July 5, 2017; Published: July 18, 2017.
DOI: 10.15376/biores.12.3.6405-6417